

Constraints of a pulsation frequency on stellar parameters in the eclipsing spectroscopic binary system: V577 Oph

O.L. Creevey^{1,2,*}, J. Telting³, J.A. Belmonte^{1,2}, T.M. Brown⁴, G. Handler⁵, T.S. Metcalfe⁶, F. Pinheiro^{7,8}, S. Sousa⁹, D. Terrell¹⁰, and A. Zhou¹¹

¹ Instituto de Astrofísica de Canarias, E-38200 La Laguna, Tenerife, Spain

² Dept. de Astrofísica, Universidad de La Laguna, E-38205 La Laguna, Tenerife, Spain

³ Nordic Optical Telescope, Apartado 474, 38700 Santa Cruz de La Palma, Spain

⁴ LCOGT Network Inc., 6740 Cortona Dr. Suite 102, Santa Barbara, CA 93117, USA

⁵ Institut für Astronomie, University of Vienna, Türkenschanzstrasse 17, A-1180 Vienna, Austria

⁶ High Altitude Observatory/National Center for Atmospheric Research, 3080 Center Green, Boulder, CO 80301, USA

⁷ Centro de Física computacional, Universidade de Coimbra, Portugal

⁸ LESIA, Observatoire de Paris, France

⁹ Centro de Astrofísica da Universidade do Porto, Rua das Estrelas, 4150-762 Porto, Portugal

¹⁰ Department of Space Studies, Southwest Research Institute, Boulder, CO, USA

¹¹ Natl. Astronomical Observatories, Chinese Academy of Sciences, 20A Datun Road, Chaoyang District, Beijing, China

Received 30 March 2010, accepted 1 April 2010

Published online later

Key words binaries: eclipsing — binaries: spectroscopic — stars: fundamental parameters — stars: oscillations — techniques: spectroscopic

We present a preliminary spectroscopic analysis of the binary system V577Oph, observed during the summer of 2007 on the 2.6m NOT telescope on La Palma. We have obtained time series spectroscopic observations, which show clear binary motion as well as radial velocity variations due to pulsation in the primary star. By modelling the radial velocities we determine a full orbital solution of the system, which yields $M_A \sin^3 i = 1.562 \pm 0.012 M_\odot$ and $M_B \sin^3 i = 1.461 \pm 0.020 M_\odot$. An estimate of inclination from photometry yields a primary mass of $\sim 1.6 M_\odot$. Using this derived mass, and the known pulsation frequency we can impose a lower limit of 1 Gyr on the age of the system, and constrain the parameters of the oscillation mode. We show that with further analysis of the spectra (extracting the atmospheric parameters), tighter constraints could be imposed on the age, metallicity and the mode parameters. This work emphasizes the power that a single pulsation frequency can have for constraining stellar parameters in an eclipsing binary system.

© 2006 WILEY-VCH Verlag GmbH & Co. KGaA, Weinheim

1 Introduction

Large amplitude δ Scuti stars are 1.5 - 2.5 M_\odot mostly MS stars, with few observed pulsation modes. Interpreting these pulsations is difficult, mainly because 1) generally, the fundamental parameters of the star are poorly constrained, and 2) we do not know enough information about the mode characteristics (degree l , azimuthal m , and radial order n) to allow us to use the mode as an extra observable constraint. To overcome these obstacles we can 1) study a pulsating star in a detached binary system, where the fundamental parameters can be determined independent of using the pulsation mode, and 2) use new techniques to study the observational profiles of the oscillations to constrain its mode properties.

V577 Oph is a detached eclipsing binary system with a δ Scuti component, and is an ideal candidate for a seismological analysis. Its orbit is eccentric ($e = 0.22$), the dominant pulsation period of the δ Scuti object is of the order of 1.3 hours, 1/100th the size of its orbital period, and the few pub-

lished light curves indicate no out-of-eclipse modulations. All of this indicates that the system is detached, and so we may assume that the δ Scuti evolves as a single star i.e. no mass transfer, tidal distortions or oscillations produced by a tidally-locked orbit.

The system was first studied by Volkov 1990. The author concluded that the primary component (the more massive and more luminous) is the pulsating star, due to the amplitude changes during primary and secondary eclipse. They also measured B-V = 0.488 mag outside of eclipse, 0.504 mag during primary eclipse minimum, and 0.509 mag during secondary eclipse minimum. Using the photometric eclipse depths, the orbital period P has been measured as 6.079 days, and a dominant pulsation frequency of 0.0695 days has been detected. The spectral types of both components have been estimated as A8 from interstellar reddening (Shugarov 1985 — referenced in Diethelm 1993), and more recently, Zhou (2001) obtained new photometric light curves and extracted the dominant pulsation frequency of 14.390 cycles per day with an oscillation amplitude of 0.029 mag.

* Corresponding author: e-mail: orlagh@iac.es

In this paper, we discuss our recent spectroscopic observations of V577Oph. As an initial analysis, we extract the radial velocities and determine the orbital parameters. Using an estimate of inclination from photometry to obtain the mass, we use seismic models to discuss the global properties of V577 Oph.

2 Observations

We obtained 5 consecutive nights on the Nordic Optical Telescope (NOT), located in the Observatorio del Roque de los Muchachos on La Palma, Canary Islands. The NOT is a 2.6m telescope with an alt-azimuth mount. The instrument used is the Fibre-fed Echelle Spectrograph (FIES) — a cross-dispersed high-resolution echelle spectrograph with a maximum resolution of $R=65,000$. Our setup was medium-resolution with $R=45,000$, with spectral range: 3640 - 7455. The maximum system efficiency (detector-instrument-fiber-telescope-atmosphere at airmass 1.0) is 9% at 6000 Å.

During the nights of July 4 - July 8, 2007 inclusive, we obtained spectra of V577 Oph, using 10 minute exposures. Accounting for calibration, *Targets of Opportunities* and other interruptions, each night an average of 32 science images in sets of 4 for V577 Oph were taken. Due to the faintness of our source ($V = 11.0$) and the potential of over-exposing ThAr, we opted to obtain the calibration frames at regular intervals of about 40-45 minutes. These frames were used to calibrate the wavelength of the two images before and after this frame. This results in a loss of accuracy in wavelength, but of the order of 0.002 \AA at $\lambda = 3659.6294 \text{ \AA}$. This corresponds approximately to an error of $0.1 - 0.2 \text{ km s}^{-1}$.

We used the `FIESTool` (Stempels, 2004)¹ reduction software to calibrate the wavelength and reduce the spectra. This tool is optimized for FIES data, but the reduction is standard and calls `IRAF` to perform some of the tasks. We subsequently shifted the spectra to barycentric frame.

3 Analysis

3.1 Determining the radial velocities

Because the spectral lines are not very broad, and the binary motion can be easily seen, we chose to measure the radial velocities by modelling a set of absorption profiles with Gaussian functions, where the central position of the Gaussian corresponds to the measured radial velocity. We identify the lines by eye, by inspecting the time series such as that shown in Fig. 1. We chose the lines that are not blended with other spectral features e.g. those around 5535 Å in Fig. 1. The lines between 5525 and 5530 Å were not chosen, because near relative radial velocities of zero, it is difficult to measure these blended lines.

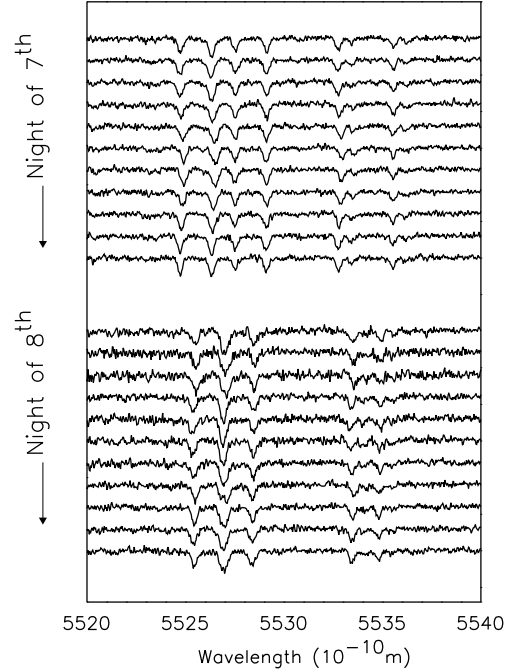


Fig. 1 Small spectral range showing the evolution of the doubled spectral lines. In some places it is clear to see the evolution of one line, while in others the lines are blended especially at maximum separation.

Figure 2 (top panel) shows the fitted radial velocities using the spectra in a range around 5183 Å as a function of phase ϕ from an arbitrary reference phase. The fitted values are shown within the dashed lines, which represent the beginning and end of one orbital period. At $\phi < 0$ and $\phi > 1$, the same data are plotted modulo Π (orbital period). The large *noise* associated with the primary component (positive radial velocities for $\phi < 0.4$) is the dominant oscillation mode with an amplitude of about 5 km s^{-1} . An initial inspection of these results indicates that the components of the system are of similar mass — the spectral features also show evidence of this.

3.2 Orbital solution

We determined the orbital solution by fitting simultaneously the free parameters: the semi-amplitude of the radial velocity curves for component *A* and *B*, K_A and K_B , the systemic velocity γ , the eccentricity e with argument of periastron ω , as a function of either time t_i or phase ϕ_i , where $\phi_i = \frac{t_i \bmod \Pi}{\Pi} - T_0$ and $T_0 = 0$ is an arbitrary reference value. When we fitted as a function of phase, the reference phase ϕ_0 was fitted with Π fixed, and when fitting with time we fitted both T_0 and Π .

We fitted the data using a χ^2 test:

$$\chi^2 = \sum_{i=1}^N \left(\frac{o_i - M_i}{\epsilon_i} \right)^2, \quad (1)$$

¹ <http://www.not.iac.es/instruments/fies/fiestool/FIESTool.html>

Table 1 Orbital Elements from Radial Velocity Curves

	P_0	P_{AB}	P_A	P_B	(σ)	P_{AB}	P_A	P_B	(σ)	P
e	0.2	0.212	0.169	0.223	(0.004)	0.204	0.167	0.224	(0.006)	0.204
γ (km s ⁻¹)	-37.0	-38.38	-38.26	-37.62	(1.34)	-38.24	-38.04	-37.66	(0.87)	-38.24
ω (°)	47.0	50.13	46.39	47.37	(0.23)	47.80	47.59	47.69	(0.22)	47.80
K_A (km s ⁻¹)	85.0	83.78	83.53	83.79	(0.60)	83.99	83.49	83.99	(0.58)	83.99
K_B (km s ⁻¹)	90.0	89.65	89.65	90.05	(0.27)	89.79	89.79	90.06	(0.35)	89.79
T_0 (days)	2.0	1.727	1.669	1.702	(0.017)	1.699	1.682	1.706	(0.01)	1.699
Π (days)	6.079	6.145	6.053	6.072	(0.030)					6.079
χ_R^2		0.649	0.691	0.523		0.672	0.687	0.520		

where o_i , ϵ_i and M_i are respectively the N observations, measurement errors and the model observables produced from a specific set of model parameters. An initial guess of the parameters are needed, and these are obtained by using the published information about the photometrically derived Π and e , and directly inspecting the radial velocity curves. The initial values are shown in the first column of Table 1. The convergence criteria was given by setting χ_R^2 (reduced χ^2) to 1 as well as testing how the free parameters changed with each iteration of the minimization algorithm. When the parameters were considered "stable" the minimization was usually stopped.

The fitting was performed by modelling the individual radial velocity curves i.e. just one of K_A and K_B and by modelling both simultaneously. These are denoted respectively in Table 1 as the column headings P_A , P_B and P_{AB} . Note that when modelling only one curve, and when the parameters converged, we fixed this solution to subsequently determine K_A or K_B from the data of the other component. The first set of columns show the results when we fitted Π and T_0 as a function of time, while the second set of columns show the results when we use phase (note that the parameter T_0 has the meaning of ϕ_0 for this second set of solutions). The fourth column lists the average value of the uncertainties from these fits.

4 Results

The fitted parameters and uncertainties (σ_i) are shown in Table 1 (see above paragraph for details). γ , ω , K_A and K_B return stable values while using all six fitting functions (data columns 2 – 4 and 6 – 8): all values fall to within their quoted uncertainties. Additionally there is no qualitative difference between these fitted parameters while leaving Π free or fixing it, the only variation found is the value of the uncertainty on γ .

The initial value of eccentricity was estimated as $e = 0.22$ (Shugarov 1985). When we fitted the radial velocities using the individual curves and then using both together we obtain very different values: 0.207, 0.168 and 0.224, with these values almost reproduced while fitting with Π fixed. Figure 2 shows the fitted radial velocity curves for each of the second three solutions. The green, red and blue curves

Table 2 Physical Stellar & Orbital Parameters

	P	σ
$M_A \sin^3 i$ (M_\odot)	1.562	0.012
$M_B \sin^3 i$ (M_\odot)	1.461	0.020
$a \sin i$ (AU)	0.0942	0.0003
Π (days)	6.0791	0.0001

show the orbital solutions from the fits using both sets of radial velocity data, the primary component only and the secondary component only, respectively. To account for the observed dominant oscillation amplitude, 5 kms⁻¹ was added to the measurement errors for the primary component for the fitting process.

Obtaining different fitted values for Π will affect the fitted value of T_0 . This is the reason that a larger difference between the T_0 values is seen for the first three solutions, than for the second three solutions. While keeping Π fixed, the variation in T_0 is only within 2σ .

Because of the large amplitude residual, it would be less feasible to regard the fit using the pulsating component data only as the optimal (red curve). Inspecting the data points (for the secondary component) and the red curve indicates that the fit is not optimal for both components. For this reason, the choice of $e = 0.16$ is discarded.

The fitted values while using the data from both stars is adopted (green curve), and are given in Table 1 last column under "P". This solution is consistent with the solution while fitting just the data from the non-pulsating component (blue). Additionally, there is no difference in the derived values of $a \sin i$, $M_A \sin^3 i$ and $M_B \sin^3 i$ when we fit Π and when it is fixed. The lower panel of Fig. 2 shows the residual for the data from the primary pulsating component divided by the observational errors (including the additional 5 km s⁻¹ added to the observed error) in red, and for the secondary component in blue. All of the data points fall to within 2ϵ indicating an adequate fit.

Using the orbital solution given under the column heading P from Table 1 we determine the system's physical parameters: $a \sin i = 0.0935 \pm 0.0003$ AU, $M_T \sin^3 i = 3.024 \pm 0.023 M_\odot$, and $q = M_B/M_A = 0.939 \pm 0.006$. Table 2 summarizes the component and orbital parameters.

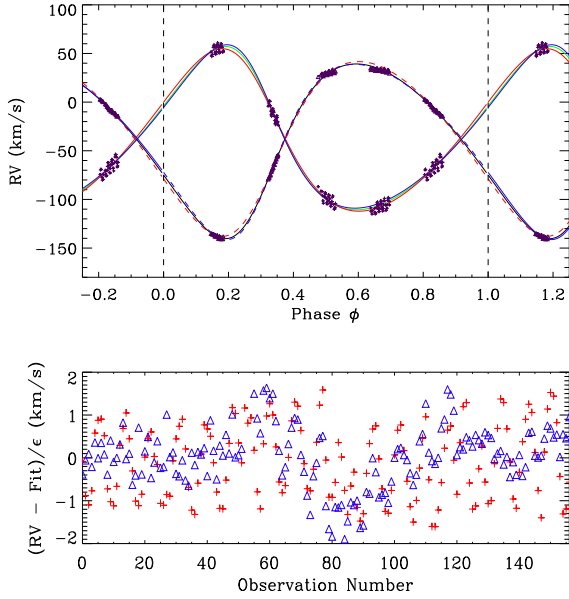


Fig. 2 *Top:* The orbital solution from fitting the radial velocity data. The data within the vertical dashed lines are the true data points, those at phase $\phi < 0$ and $\phi > 1$ are the data repeated modulo II. The green, red and blue curves represent the resulting fit curves from P_B , P_A and P_{AB} . *Bottom:* Residual of data minus fit radial velocity curve with P_{AB} for the primary (red) and the secondary (blue).

5 Seismic inference

An estimate of the inclination of the system from photometry ($i > 80^\circ$) yields a primary mass of $\sim 1.6 M_\odot$ (Zhou, priv. comm.). Figure 3 show theoretical frequencies of a $1.63 M_\odot$ star for 2 values of metallicity: Z (initial metal mass fraction) = 0.020 and 0.025. These mode frequencies were calculated using the ASTEC and ADIPLS stellar structure, evolution and pulsation codes (Christensen-Dalsgaard 2008a,b). The lines correspond to fundamental (continuous) and first overtone (dashed) oscillation modes of different degree ($l = 0, 1, 2$ from bottom to top). The boxes represent the observed value of the frequency which includes an error to take into account that the frequency could have a non-zero azimuthal order (m where $-l < m < l$).

If we assume that no g-modes are present, since these are not common among large amplitude δ Scuti stars, Figure 3 then shows that the system must have a lower age limit of 1 Gyr (younger stars exhibit higher frequencies). If we knew which mode was observed we could further constrain the age to either 1.2 – 1.3 Gyr or 1.6 – 2.0 Gyr. Also we see that there are three possible solutions to the identity of the mode, without using any observational technique to do this. These possibilities are: radial mode (fundamental or first overtone) or fundamental non-radial mode $l = 1$. We can also see that a metallicity measurement and a mode-

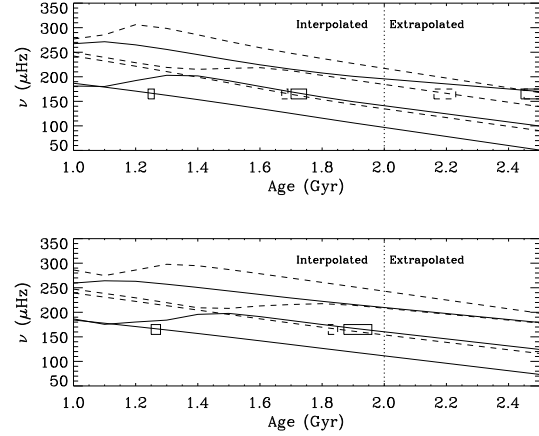


Fig. 3 Frequency values for various low degree modes for a $1.63 M_\odot$ star (V577 Oph A) as a function of age for $Z = 0.020$ (top) and 0.025 (bottom). See text for details.

identification would provide further constraints on the age and chemical composition.

6 Conclusions

We obtained 5 nights of spectroscopic observations of the eclipsing binary with a δ Scuti component V577 Oph. We extracted the radial velocities of both components, which shows very clear orbital motion of both stars and pulsations in the primary (more massive) star. We fitted the velocities to solve for the orbital parameters and then derive for the components $M_A \sin^3 i = 1.562 \pm 0.012 M_\odot$ and $M_B \sin^3 i = 1.461 \pm 0.020 M_\odot$. An estimate of inclination implies a primary pulsating component of $\sim 1.6 M_\odot$.

A dominant oscillation frequency has been confirmed, and comparing this with some stellar evolution and pulsation models allows us to impose a lower limit of 1 Gyr on the age of the star, and constrains the identification of the mode to either radial mode (fundamental or first overtone) or fundamental non-radial mode $l = 1$. We plan to disentangle the spectra in order to determine the atmospheric parameters of T_{eff} , $[M/H]$, and $\log g$. This information would additionally constrain both the age of the star and the pulsation mode parameters.

Acknowledgements. This data has been collected using the NOT telescope operated at the Observatorio del Roque de los Muchachos on the island of La Palma, Canary Islands. This work was partially funded by a Newkirk Graduate Research grant at the High Altitude Observatory, Boulder, Colorado, USA. F.J.G.P. acknowledges grant /SFRH/BPD/37491/2007 from F.C.T.

References

- Christensen-Dalsgaard, J. 2008a, Ap&SS, 316, 113
- Christensen-Dalsgaard, J. 2008b, Ap&SS, 316, 13
- Shugarov, S. Y. 1985, Astronomicheskij Tsirkulyar, 1359, 4
- Volkov, I. M. 1990, IBVS, 3493, 1

Zhou, A.-Y. 2001, IBVS, 5087, 1
Diethelm, R. 1993, IBVS, 3894, 1